The Preparation of *t*-Butyl Acrylate, Methyl Acrylate, and Styrene Block Copolymers by Atom Transfer Radical Polymerization: Precursors to Amphiphilic and Hydrophilic Block Copolymers and Conversion to Complex Nanostructured Materials

QINGGAO MA, KAREN L. WOOLEY

Department of Chemistry, Washington University, One Brookings Drive, St. Louis, Missouri 63130-4899

Received 4 August 2000; accepted 8 September 2000

ABSTRACT: Atom transfer radical polymerization conditions with copper(I) bromide/pentamethyldiethylenetriamine (CuBr/PMDETA) as the catalyst system were employed for the polymerization of *tert*-butyl acrylate, methyl acrylate, and styrene to generate well-defined homopolymers, diblock copolymers, and triblock copolymers. Temperature studies indicated that the polymerizations occurred smoothly in bulk at 50 °C. The kinetics of *tert*-butyl acrylate polymerization under these conditions are reported. Well-defined poly(*tert*-butyl acrylate) (P*t*BA; polydispersity index = 1.14) and poly(methyl acrylate) (PMA; polydispersity index = 1.03) homopolymers were synthesized and then used as macroinitiators for the preparation of P*t*BA-*b*-PMA and PMA-*b*-P*t*BA diblock copolymers in bulk at 50 °C or in toluene at 60 or 90 °C. In toluene, the amount of CuBr/PMDETA relative to the macroinitiator was important; at least 1 equiv of CuBr/PMDETA was required for complete initiation. Typical block lengths were composed of 100–150 repeat units per segment. A triblock copolymer, composed of P*t*BA-*b*-PMA-*b*-PS (PS = polystyrene), was also synthesized with a well-defined composition and a narrow molecular weight dispersity. The *tert*-butyl esters of P*t*BA-*b*-PMA and P*t*BA-*b*-PMA-*b*-PS were selectively cleaved to form the amphiphilic block copolymers PAA-*b*-PMA [PAA = poly(acrylic acid)] and PAA-*b*-PMA-*b*-PS, respectively, via reaction with anhydrous trifluoroacetic acid in dichloromethane at room temperature for 3 h. Characterization data are reported from analyses by gel permeation chromatography; infrared, ^{1}H NMR, and ^{13}C NMR spectroscopies; differential scanning calorimetry; and matrix-assisted, laser desorption/ionization time-of-flight mass spectrometry. The assembly of the amphiphilic triblock copolymer PAA_{90}-*b*-PMA_{80}-*b*-PS_{98} within an aqueous solution, followed by conversion into stable complex nanostructures via crosslinking reactions between the hydrophilic PAA chains comprising the peripheral layers, produced mixtures of spherical and cylindrical topologies. The visualization and size determination of the resulting nanostructures were performed by atomic force microscopy, which revealed very interesting segregation phenomena. © 2000 John Wiley & Sons, Inc. J Polym Sci A: Polym Chem 38: 4805–4820, 2000

Keywords: atom transfer radical polymerization (ATRP); pentamethyldiethylenetriamine (PMDETA); *tert*-butyl acrylate; methyl acrylate; styrene; amphiphilic block copolymer; triblock copolymer; shell crosslinked nanostructures

INTRODUCTION

Block copolymers composed of segments with different solubility properties have been of considerable interest because of their ability to self-assemble in solution or bulk states. The self-assembly carried out in solution allows for the preparation of individual nanoscopic materials generally possessing a core–shell morphology and being spherically, cylindrically, or vesicularly shaped.[1,2] The assembly of amphiphilic diblock or triblock copolymers within an aqueous solution

---

Correspondence to: K. L. Wooley (E-mail: klwooley@artsci.wustl.edu)

Journal of Polymer Science: Part A: Polymer Chemistry, Vol. 38, 4805–4820 (2000)

has been followed by crosslinking reactions selectively throughout the core[3] or shell[4–10] domains to afford stable nanoscale particles. These complex nanostructures have shown promise for utilization in environmental, biomedical, and materials applications, including the sequestration of pollutants, drug delivery, gene therapy, coatings, and composites.[11–14]

The crucial component in each of the supramolecular assemblies and their stabilized, crosslinked counterparts is the nature of the block copolymers, the molecular weight and composition of which dictate the kinetics and thermodynamics of their organization. We focused on amphiphilic diblock copolymers, in which one of the blocks is poly(acrylic acid) (PAA). This allows for the preparation of shell-crosslinked (SCK) nanoparticles in an aqueous solution with amidation of the acrylic acid groups as the means for crosslinking of the polymer micelle peripheral layer; it also provides materials of the appropriate morphology to be utilized in water.[15] The core compositions and properties in previous examples of SCK nanoparticles have included mainly hydrophobic chain segments, such as glassy polystyrene (PS),[9,15] fluidlike poly(isoprene),[16] and crystalline poly(ϵ-caprolactone).[17] The incorporation of *N*-(morpholino)ethyl methacrylate as the core material generated quite interesting structures with temperature-variable core hydrophilicity.[5] This prompted us to develop an SCK structure based entirely on hydrophilic PAA, in which the establishment of an acrylamido-crosslinked network throughout the shell layer would maintain the three-dimensional architecture. To accomplish the assembly process, however, hydrophobic precursors are needed for core nucleation within an aqueous environment. Therefore, a block copolymer of acrylic acid segments for shell formation and crosslinking chemistry must be linked covalently to an acrylate ester segment for core nucleation and organization of the nanoassembly.

Although anionic polymerization is an excellent method for the preparation of well-defined block copolymers, it is technically challenging and not compatible with electrophilic or acidic functional groups. Free-radical polymerization can be used more broadly with monomers containing functionalities; however, it was not amenable to the preparation of well-defined polymers, especially block copolymers, until the recent breakthroughs in living free-radical polymerization chemistries, including transition-metal-mediated radical polymerization,[18,19] atom transfer radical polymerization (ATRP),[20–23] nitroxide-mediated radical polymerization,[24–26] and reversible addition fragmentation transfer polymerization.[27–30] ATRP has been successfully employed for the polymerization of a variety of acrylate monomers, such as methyl acrylate (MA),[31,32] *n*-butyl acrylate,[23] and 2-hydroxyethyl acrylate.[33] Under copper-mediated ATRP conditions, polymerization is initiated by an alkyl halide,[34–38] and the reversible homolytic bond cleavage of the alkyl halide group is facilitated by the redox properties of the copper species as a complex with bidentate or multidentate *N*-containing ligands. Among these ligands, 4,4′-di-*n*-heptyl-2, 2′-bipyridine and 4,4′-di-(5-nonyl)-2,2′-bipyridine have been used extensively.[20,23,34–38] Because these are not commercially available and are relatively expensive to synthesize, the preparation of large amounts of well-defined block copolymers from these ligands is hindered. Polymerization in the presence of multidentate alkyl amino ligands, such as pentamethyldiethylenetriamine (PMDETA), has been found to proceed at faster rates and lower temperatures.[31] Moreover, PMDETA is commercially available and much less expensive than the bipyridine derivatives and, thus, deserves further study. Recently, Matyjaszewski et al.[39,40] reported the polymerization of *tert*-butyl acrylate (*t*BA) with the CuBr/PMDETA system. This chemistry has also allowed for the preparation of diblock copolymers of PS and PAA.[41] Because the catalyst is heterogeneous in bulk *t*BA monomer, various polymerization conditions were attempted to determine the optimal conditions for the polymerization. In particular, the addition of *p*-dimethoxybenzene, acetone, or *N,N*-dimethylformamide as a solvent, together with a 5% excess of $CuBr_2$ relative to CuBr to moderate the reaction rate, was found to produce the best results. Reduced temperatures (55 °C or room temperature) in bulk were found to result in slow polymerization rates and broad molecular weight dispersities.

In this article, we report the preparation of diblock and triblock copolymers of *t*BA, MA, and styrene by ATRP. These block copolymers have the potential for segment-selective removal of the ester protecting group because of the reactivity differences associated with *tert*-butyl and methyl ester groups and, therefore, serve as versatile polymer precursors for the preparation of amphiphilic and entirely hydrophilic nanostructured materials. The ATRP-based polymerizations of *t*BA and MA were studied, and it was found that the polymerizations could be accomplished on a large scale in bulk, without the addition of solvent. By lowering the polymerization temperature to 50 °C and carefully controlling the polymerization procedure to minimize the oxidation of Cu(I) to Cu(II), we obtained well-behaved polymerizations occurring at reasonable rates to yield well-defined polymers of narrow molecular weight dispersities. The initially prepared homopolymers then served as macroinitiators for the growth of diblock and triblock copolymers from combinations of *t*BA, MA, and styrene monomers. Selective cleavage of the *tert*-butyl ester groups produced acrylic acid chain segments and converted the hydrophobic materials into amphiphilic diblock or triblock copolymers. The amphiphilic triblock copolymers proved to be of particular interest, in that they underwent self-assembly in water to form cylindrically shaped nanoassemblies, in addition to the common spherical nanospheres. These assemblies were transformed into stable and robust nanostructures by intra-assembly crosslinking within the hydrophilic shell layers through amidation of the acrylic acid groups after the reaction with diamino crosslinking agents. These nanostructures remained suspended in an aqueous solution indefinitely and organized into unusual ordered arrays after transfer onto a substrate by deposition and drying of the aqueous solutions.

EXPERIMENTAL

Measurements

IR spectra were obtained on a PerkinElmer Spectrum BX Fourier transform infrared as diffuse reflectance. ^{1}H NMR spectra were recorded as solutions on either a Varian Unity 300-MHz spectrometer or a Varian Gemini 300-MHz spectrometer with the solvent proton signal as a standard. ^{13}C NMR spectra were recorded at 75.4 MHz as solutions on either a Varian Unity 300 spectrometer or on a Varian Gemini 300 spectrometer with the solvent carbon signal as a standard.

Gel permeation chromatography (GPC) was conducted on a Hewlett–Packard series 1050 High Performance Liquid Chromatograph (HPLC) with a Hewlett–Packard 1047A refractive index detector: data analysis was done with Viscotek (Houston, TX) Trisec GPC Software (version 2.70). PS was used as a standard. Two 5-μm Polymer Laboratories PL gel columns (300 × 7.7 mm) connected in series in order of increasing pore size (500 Å, mixed-bed E) were used with tetrahydrofuran (THF) distilled from CaH_2 as a solvent. Glass-transition temperatures (T_g) were measured by differential scanning calorimetry on a PerkinElmer DSC-4 differential scanning calorimeter. Heating rates were 10 °C/min, and the T_g was taken as the midpoint of the inflection tangent after the third or subsequent heating scan. The PerkinElmer instrument was upgraded with an Instrument Specialists, Inc. (Antioch, IL) temperature program interface-PE, and data were acquired and analyzed with TA-PC software (version 2.11; Instrument Specialists).

Tapping-mode atomic force microscopy (AFM) observations were carried out in air with a Nanoscope III BioScope system (Digital Instruments, Santa Barbara, CA) operated under ambient conditions with standard silicon tips (type, OTESPA-70; L, 160 μm; normal spring constant ,50 N/m; resonance frequency, 246–282 kHz). We prepared the samples for AFM analysis by depositing a 1-μL drop of the solution (5–500 μg/mL) onto mica and allowing it to dry freely in air.

The MALDI-TOF (matrix-assisted laser desorption/ionization time-of-flight) experiments were carried out on a Voyager DE-RP (Perseptive Biosystems, Framingham, MA). A mixture of 2,4,6-trihydroxyacetophenone, 2,3,4-trihydroxyacetophenone, and ammonium citrate (Sigma, St. Louis, MO) at a 2/1/2 molar ratio, with a 2,4,6-trihydroxyacetophenone concentration of 0.05 M, was used as the matrix. Samples were dissolved in THF at a concentration of 10 pmol/μL. A 0.5-μL sample aliquot and 0.5 μL of the matrix solution were mixed on a stainless steel plate. Both negative and positive ions were desorbed with an N_2 laser (337 nm) and accelerated with a potential of 25 kV. The data were collected with a Tektronics TDS 520A digitizing oscilloscope (Tektronics, Beaverton, OR), transferred to the computer, and processed with Perseptive Grams/386 (version 3.04; Perseptive Biosystems) software.

Materials

Nitrogen (99.99%) was used for the polymerization and storage of materials. Argon (99.99%) was used during the transfer of reagents inside an air bag. THF (Aldrich; 99%) and toluene were distilled from calcium hydride. MA (Aldrich; 99%), *t*BA (Aldrich; 98%), and styrene (Aldrich; 99%) were distilled from calcium hydride and stored under N_2 at −20 °C. Copper(I) bromide (CuBr; Aldrich; 99.999%), copper(I) chloride (Aldrich; 99.999%), ethyl 2-bromopropionate (2-EBP; Aldrich; 99%), (1-bromoethyl)benzene (Aldrich; 97%), ethyl 2-bromoisobutyrate (2-EB*i*B; Aldrich; 98%), and *N,N,N′,N″,N″*-pentamethyldiethylenetriamine (PMDETA; Aldrich; 99%) were used as received.

General Procedure for the Polymerization of *t*BA in Bulk

A 250-mL Schlenk flask fitted with a stir bar (oven-dried at 110 °C for 48 h and flame-dried under vacuum immediately prior to use) and covered with a rubber septum was charged with CuBr (981 mg, 6.84 mmol) under argon in an air bag. The Schlenk flask was connected to a condenser and a double manifold. The flask was evacuated (0.1 mmHg) for 15 min, backfilled with N_2, and then immersed in liquid N_2. *t*BA (100 mL, 87.5 g, 684 mmol) was added via a gas-tight syringe, followed by PMDETA (1.43 mL, 1.19 g, 6.84 mmol). After three freeze–pump–thaw cycles, the Schlenk flask was then immersed again in liquid N_2. 2-EBP (900 μL, 1.24 g, 6.84 mmol) was added to the flask via a gas-tight syringe. Three freeze–pump–thaw cycles were performed, and the mixture was allowed to stir at room temperature for 10 min to ensure that the mixture became homogeneous. The flask was then placed into a 50 °C oil bath to allow for polymerization under N_2. Periodically, 0.2-mL aliquots were removed via a gas-tight syringe for GPC analysis. After completion of the reaction, the flask was immersed in liquid N_2 to quench the polymerization. THF (100 mL) was then added to the flask, and a vortex technique was used to dissolve the polymer. The mixture was then filtered through a 150-mL fritted Buchner funnel containing an Al_2O_3/celite plug to remove the copper. The resulting colorless polymer solution was concentrated and twice precipitated into 70% methanol/water (2 L) at 4 °C. The white polymer was collected by vacuum filtration and dried under vacuum for 3 days at room temperature to give poly(*tert*-butyl acrylate) (P*t*BA).

Yield: 70 g (80%). $M_n^{\mathrm{NMR}} = 8000$ g/mol, $M_n^{\mathrm{GPC}} = 11{,}600$ g/mol, $M_w/M_n = 1.17$. $T_g = 34$ °C. IR: 755, 844, 1157, 1256, 1366, 1443, 1723, 2975, 3434 cm^{-1}. ^{1}H NMR (CDCl$_3$, δ): 1.05 (d, C**H**$_3$CH end group), 1.22 (t, C**H**$_3$CH$_2$O end group), 1.20–1.50 (br, (C**H**$_3$)$_3$C), 1.24–1.68 (br, meso and racemo C**H**$_2$ of the polymer backbone), 1.74–1.94 (br, meso C**H**$_2$ of the polymer backbone), 2.15–2.35 (br, C**H** of the polymer backbone), 4.05 (m, CH$_3$C**H**$_2$O and C**H**Br end groups overlapping) ppm. ^{13}C NMR (CDCl$_3$, δ): 27.9–28.0 [(**C**H$_3$)$_3$C], 35.7–37.2 (β carbon of the polymer backbone), 41.7–42.2 (α carbon of the polymer backbone), 80.2 [(CH$_3$)$_3$**C**], 173.6–173.8 (carbonyl C) ppm. Elem. Anal. Calcd. for $C_{434}H_{744}BrO_{124}$ (8000 g/mol, number average degree of polymerization = 62 by ^{1}H NMR): C, 64.94%; H, 9.35%; Br, 1.00%. Calcd. for $C_{630}H_{1080}BrO_{180}$ (11,600 g/mol, DP$_n$ = 90 by GPC): C, 65.15%; H, 9.37%; Br, 0.69%. Found: C, 64.87%; H, 9.35%; Br, 0.81%.

General Procedure for the Polymerization of MA in Bulk

A 250-mL Schlenk flask fitted with a stir bar (oven-dried at 110 °C for 48 h and flame-dried under vacuum immediately prior to use) and covered with a rubber septum was charged with CuBr (1.33 g, 9.25 mmol) under argon in an air bag. The Schlenk flask was connected to a condenser and a double manifold. The flask was evacuated (0.1 mmHg) for 15 min, backfilled with N_2, and then immersed in liquid N_2. MA (125 mL, 120 g, 1390 mmol) was added via a gas-tight syringe, followed by PMDETA (2.00 mL, 1.60 g, 9.25 mmol). After three freeze–pump–thaw cycles, the Schlenk flask was then immersed again in liquid N_2. 2-EBP (1.20 mL, 1.68 g, 9.25 mmol) was added to the flask via a gas-tight syringe. Three freeze–pump–thaw cycles were performed, and then the mixture was allowed to stir at room temperature for 10 min to ensure that the mixture became homogeneous. The flask was then placed into a 50 °C oil bath to allow for polymerization under N_2. Periodically, 0.2-mL aliquots were removed via a gas-tight syringe for GPC analysis. The flask was immersed in liquid N_2 to quench the polymerization. THF (50 mL) was then added to the flask, and the mixture was filtered through a 150-mL fritted Buchner funnel containing an Al_2O_3/celite plug to remove the copper. The resulting colorless polymer solution was concentrated and precipitated twice into 70% methanol/water (2 L) at 4 °C, and the supernatant was decanted. The precipitate was dried under vacuum at room temperature for 3 days to give poly(methyl acrylate) (PMA) as a colorless glass.

Yield: 65 g (54%). MALDI-TOF (3-indoleacrylic acid doped with AgOAc as a matrix): $M_n = 8598$ g/mol, $M_w/M_n = 1.030$. $M_n^{\mathrm{NMR}} = 8800$ g/mol, $M_n^{\mathrm{GPC}} = 9110$ g/mol, $M_w/M_n = 1.04$. $T_g = 11$ °C. IR: 756, 826, 967, 1069, 1256, 1443, 1728, 2024, 2960, 3440, 3643 cm^{-1}. ^{1}H NMR (CDCl$_3$, δ): 1.05 (d, C**H**$_3$CH end group), 1.22 (t, C**H**$_3$CH$_2$O end group), 1.28–1.62, 1.76–2.0 (br, meso C**H**$_2$ of the polymer backbone), 1.62–1.76 (br, racemo C**H**$_2$ of the polymer backbone), 2.15–2.38 (br, C**H** of the polymer backbone), 3.62 (s, OC**H**$_3$), 4.08 (q, OC**H**$_2$CH$_3$ end group), 4.15 (t, C**H**Br end group) ppm. ^{13}C NMR (CDCl$_3$, δ): 35.7–37.2 (β carbon of the polymer backbone), 41.8–42.2 (α carbon of the polymer backbone), 51.6 ($O\mathbf{C}H_3$), 174.5 (carbonyl C) ppm. ELEM. ANAL. Calcd. for $C_{404}H_{606}BrO_{202}$ (8800 g/mol, DP_n = 102 by ^{1}H NMR): C, 55.30%; H, 6.96%; Br, 0.92%. Calcd. for $C_{412}H_{618}BrO_{206}$ (9110 g/mol, DP_n = 105 by GPC): C, 55.32%; H, 6.99%; Br, 0.88%. Found: C, 55.50%; H, 6.98%; Br, 0.71%.

General Procedure for the Preparation of P*t*BA-*b*-PMA in Bulk

A 100-mL Schlenk flask fitted with a stir bar (oven-dried at 110 °C for 48 h and flame-dried under vacuum immediately prior to use) and covered with a rubber septum was charged with P*t*BA as a macroinitiator (M_n = 11,600, M_w/M_n = 1.17; 10 g, 0.86 mmol). The flask was evacuated (0.1 mmHg) for 15 min and then backfilled with N_2. CuBr (372 mg, 2.59 mmol, 3.0 equiv to the macroinitiator) was added under argon in an air bag. The Schlenk flask was connected to a condenser and a double manifold. The flask was evacuated (0.1 mmHg) for another 15 min, backfilled with N_2, and then immersed in liquid N_2. MA (40.0 mL, 38.2 g, 444 mmol, 515 equiv to the macroinitiator) was added via a gas-tight syringe. After three freeze–pump–thaw cycles, the mixture was allowed to stir at room temperature for 20 min and then was immersed again in liquid N_2. PMDETA (541 μL, 450 mg, 2.59 mmol) was added via a gas-tight syringe, followed by three freeze–pump–thaw cycles, and the mixture was then allowed to stir at room temperature for 10 min to ensure that the mixture became homogeneous. The flask was then placed into a 50 °C oil bath to allow for polymerization under N_2. Periodically, 0.1-mL aliquots were removed via a gas-tight syringe for GPC analysis. The flask was immersed in liquid N_2 to quench the polymerization. THF (50 mL) was then added to the flask, and the mixture was filtered through a 150-mL fritted Buchner funnel containing an Al_2O_3/celite plug to remove the copper. The resulting colorless solution was then concentrated and precipitated twice in 70% methanol/water (1 L) at 4 °C. The resulting polymer was collected by vacuum filtration and dried under vacuum at room temperature for 3 days to give P*t*BA-*b*-PMA diblock polymer.

Yield: 15 g (31%). MALDI-TOF (3-indoleacrylic acid doped with AgOAc as a matrix): M_n = 14,875 g/mol, M_w/M_n = 1.09. M_n^{NMR} = 13,000 g/mol, M_n^{GPC} = 18,500, M_w/M_n = 1.13. $(T_g)_{\mathrm{PMA}}$ = 14 °C, $(T_g)_{\mathrm{P}t\mathrm{BA}}$ = 44 °C. IR: 752, 845, 1187, 1451, 1992, 2966, 3440, 3643 cm^{-1}. ^{1}H NMR ($CDCl_3$, δ): 1.24–1.74 (br, $C\mathbf{H}_2$ of the polymer backbone), 1.20–1.50 [br, $(C\mathbf{H}_3)_3C$], 1.76–1.94 (br, $C\mathbf{H}_2$ of the polymer backbone), 2.15–2.35 (br, C**H** of the polymer backbone), 3.50–3.65 (br, $OC\mathbf{H}_3$) ppm. ^{13}C NMR ($CDCl_3$, δ): 27.9–28.0 [$(\mathbf{C}H_3)_3C$], 34.8–37.2 (β carbon of the polymer backbone), 41.1–42.2 (α carbon of the polymer backbone), 51.6 ($O\mathbf{C}H_3$), 80.2 [$(CH_3)_3\mathbf{C}$], 174.5 (carbonyl C from PMA block), 174.6 (carbonyl C from P*t*BA block) ppm.

General Procedure for the Preparation of PMA-*b*-P*t*BA in Toluene

PMA macroinitiator (M_n^{GPC} = 9110 g/mol, M_w/M_n = 1.04) was frozen in liquid N_2 to facilitate the transfer of a portion (11.0 g, 1.22 mmol) into a 100-mL Schlenk flask fitted with a stir bar (oven-dried at 110 °C for 48 h and flame-dried under vacuum immediately prior to use) and covered with a rubber septum. The flask was evacuated (0.1 mmHg) for 1 h to remove the condensed moisture. CuBr (263 mg, 1.85 mmol, 1.52 equiv) was added under argon in an air bag. The flask was immersed in liquid N_2, and toluene (20 mL) and *t*BA (20.0 mL 17.5 g, 137 mmol) were added via a gas-tight syringe. After three freeze–pump–thaw cycles, the mixture was allowed to stir at room temperature for 1 h to ensure that the mixture became homogeneous. The flask was then immersed into liquid N_2, and PMDETA (400 μL, 318 mg, 1.83 mmol, 1.51 equiv) was added via a gas-tight syringe. After three freeze–pump–thaw cycles, the flask was placed into a 90 °C oil bath to allow the polymerization to proceed. After completion of the reaction, the flask was immersed in liquid N_2 to quench the polymerization. THF (40 mL) was added, and the solution was filtered through a 150-mL fritted Buchner funnel containing an Al_2O_3/celite plug to remove the copper. The colorless filtrate was concentrated under reduced pressure and precipitated twice into 70% methanol/water (1 L) at 4 °C. The white polymer was collected by vacuum filtration and dried under vacuum for 3 days to give PMA-*b*-P*t*BA as a white solid.

Yield: 14 g (49%). M_n^{NMR} = 12,640 g/mol, M_n^{GPC} = 18,700 g/mol, M_w/M_n = 1.17. $(T_g)_{\mathrm{PMA}}$ = 11 °C, $(T_g)_{\mathrm{P}t\mathrm{BA}}$ = 44 °C. IR: 752, 845, 1187, 1451, 1992, 2966, 3440, 3643 cm^{-1}. ^{1}H NMR ($CDCl_3$, δ): 1.24–1.74 (br, $C\mathbf{H}_2$ of the polymer backbone), 1.25–1.50 [br, $(C\mathbf{H}_3)_3C$], 1.76–1.94 (br, $C\mathbf{H}_2$ of the polymer backbone), 2.15–2.35 (br, C**H** of the polymer backbone), 3.50–3.62 (br, $OC\mathbf{H}_3$) ppm. ^{13}C NMR ($CDCl_3$, δ): 27.9–28.0 [$(\mathbf{C}H_3)_3C$], 34.8–37.2 (β carbon of the polymer backbone), 41.0–42.2 (α carbon of the polymer backbone), 51.6 (O**C**H_3), 80.2 [$(CH_3)_3$**C**], 173.6–173.8 (carbonyl C from the P*t*BA block), 174.5 (carbonyl C from the PMA block) ppm. Elem. Anal. Calcd. for $C_{612}H_{996}BrO_{228}$[12,640 g/mol, $(DP_n)_{PMA}$ = 102, $(DP_n)_{PtBA}$ = 30 by ^1H NMR]: C, 61.20%; H, 8.30%. Calcd. for $C_{973}H_{1602}BrO_{344}$ [18,700 g/mol, $(DP_n)_{PMA}$ = 105, $(DP_n)_{PtBA}$ = 75 by GPC]: C, 62.43%; H, 8.57%. Found: C, 62.26%; H, 8.70%.

General Procedure for the Conversion of P*t*BA-*b*-PMA to PAA-*b*-PMA

A clean, 100-mL, round-bottom flask fitted with a stir bar was charged with P*t*BA-*b*-PMA (M_n^{GPC} = 18,500, M_w/M_n = 1.11; 3.0 g, 12.5 mmol of *tert*-butyl ester), followed by dichloromethane (30 mL). The mixture was allowed to stir for 10 min to dissolve the polymer. Trifluoroacetic acid (TFA; 5.0 mL, 7.4 g, 65 mmol, 5.0 equiv to the *tert*-butyl ester) was then added. After the mixture was allowed to stir at room temperature for 12 h, the dichloromethane and excess TFA were removed at room temperature with dry air gently flowing through the flask overnight. The resulting glassy, light-brown polymer solid was vacuum-dried for 2 days to give PAA-*b*-PMA (2.5-g yield). For further purification, the polymer was dissolved in THF (20 mL), transferred into dialysis tubing (molecular weight cut-off ~ 3500), and dialyzed against deionized water for 3 days. Lyophilization gave PAA-*b*-PMA as a white powder.

Yield: 2.0 g (100%). $(T_g)_{PMA}$ = 11 °C, $(T_g)_{PAA}$ = 114 °C. IR: 602, 821, 1053, 1179, 1273, 1447, 1663, 1752, 2400–3513 cm^{-1}. ^1H NMR (CD_2Cl_2, δ): 1.12–1.87 (br, C**H_2** of the polymer backbone), 2.15–2.45 (br, C**H** of the polymer backbone), 3.50–3.62 (br, OC**H_3**) ppm. ^{13}C NMR (CD_3OD/$CDCl_3$, δ): 34.2 (β carbon of the polymer backbone), 40.7 (α carbon of the polymer backbone), 48.5 (O**C**H_3), 174 (carbonyl C from PMA block), 177 (carbonyl C from PAA block) ppm. Elem. Anal. Calcd. for $C_{574}H_{826}BrO_{322}$ [9300 g/mol, $(DP_n)_{PMA}$ = 62, $(DP_n)_{PtBA}$ = 56 by ^1H NMR]: C, 53.40%; H, 6.40%. Calcd. for $C_{581}H_{824}BrO_{338}$ [16,100 g/mol, $(DP_n)_{PMA}$ = 90, $(DP_n)_{PtBA}$ = 80 by GPC]: C, 52.8%2; H, 6.24%. Found: C, 50.22%; H, 6.03%.

General Procedure for the Preparation of P*t*BA-*b*-PMA-*b*-PS in Bulk

A 50-mL Schlenk flask fitted with a stir bar (oven-dried at 110 °C for 48 h and flame-dried under vacuum immediately prior to use) and covered with a rubber septum was charged with P*t*BA-*b*-PMA [M_n = 18,500, polydispersity index (PDI) = 1.13; 1.0 g, 0.054 mmol] and CuBr (30 mg, 0.21 mmol) under argon in an air bag. The Schlenk flask was connected to a condenser and a double manifold. The flask was evacuated (0.1 mmHg) for 15 min, backfilled with N_2, and then immersed in liquid N_2. Styrene (10 mL, 9.1 g, 87 mmol) was added via a gas-tight syringe. After three freeze–pump–thaw cycles, the Schlenk flask was then immersed again in liquid N_2. PMDETA (40 μL, 36 mg, 0.21 mmol) was added via a gas-tight syringe. Three freeze–pump–thaw cycles were performed, and the mixture was allowed to stir at room temperature for 10 min to ensure that the mixture became homogeneous. The flask was then placed into a 50 °C oil bath to allow for polymerization under N_2. Periodically, 0.1-mL aliquots were removed via a gas-tight syringe for GPC analysis. After completion of the reaction, the flask was immersed in liquid N_2 to quench the polymerization. THF (40 mL) was then added to the flask, and the mixture was filtered through a 50-mL fritted Buchner funnel containing an Al_2O_3/celite plug to remove the copper. The resulting colorless polymer solution was concentrated and precipitated twice into 80% methanol/water (1 L) at 4 °C. The precipitate was collected by vacuum filtration and dried under vacuum for 3 days to give P*t*BA-*b*-PMA-*b*-PS as a white solid.

Yield: 1.2 g (12%). M_n^{NMR} = 20,000 g/mol, M_n^{GPC} = 28,700 g/mol, M_w/M_n = 1.16. IR: 473, 543, 700.3, 757, 845, 1164, 1256, 1370, 1448, 1600, 1738, 1946, 2929, 3441, 4049 cm^{-1}. ^1H NMR ($CDCl_3$, δ): 1.20–2.00 (br, polymer backbone), 1.25–1.50br, [(C**H_3**)$_3$C], 2.00–2.42 (br, polymer backbone), 3.50–3.64 (br, OC**H_3**), 6.26–6.84 (br, meta-H from the aromatic ring), 6.84–7.22 (br, ortho- and para-H from the aromatic ring) ppm. ^{13}C NMR ($CDCl_3$, δ): 27.9–28.0 [(**C**H_3)$_3$C], 34.9–37.3 (β carbon of the polymer backbone), 40.3–42.3 (α carbon of the polymer backbone), 51.7 (O**C**H_3), 80.4 [$(CH_3)_3$**C**], 126, 128, 145, 174 (carbonyl C from the P*t*BA block), 175 (carbonyl C from the PMA block). Elem. Anal. Calcd. for $C_{1194}H_{1616}BrO_{236}$ [20,000 g/mol, $(DP_n)_{PMA}$ = 62, $(DP_n)_{PtBA}$ = 56, $(DP_n)_{PS}$ = 67 by ^1H NMR]: C, 71.64%; H, 8.08%. Calcd. for $C_{1734}H_{2344}BrO_{340}$ [28,700 g/mol, $(DP_n)_{PMA}$ = 90, $(DP_n)_{PtBA}$ = 80, $(DP_n)_{PS}$ = 98 by GPC]: C, 72.50%; H, 8.17%. Found: C, 72.42%; H, 8.18%.

General Procedure for Micelle Formation from PAA-*b*-PMA-*b*-PS

A 500-mL, round-bottom flask fitted with a stir bar was charged with PAA_{90}-*b*-PMA_{80}-*b*-PS_{98} (M_n

= 24,000 g/mol, PDI = 1.16; 120 mg, 0.56 mmol for acrylic acid groups). THF (50 mL, distilled from CaH_2) was added, and the solution was allowed to stir at room temperature for 10 min to ensure that the mixture became homogeneous. Nanopure water (70 mL, 18 MΩ cm^{-1}) was added via a syringe pump at a rate of 15 mL/h. After all the water was added, the bluish micelle solution was transferred to dialysis tubing (MWCO = 6000–8000) and dialyzed against deionized water for 48 h to remove all the THF. The final volume was about 240 mL, giving a polymer concentration of about 0.51 mg/mL.

General Procedure for the Formation of SCK Nanostructures from PAA-*b*-PMA-*b*-PS

A 250-mL, round-bottom flask fitted with a stir bar was charged with a PAA$_{90}$-*b*-PMA$_{80}$-*b*-PS$_{98}$ micelle solution (160 mL, ~0.51 mg/mL, 0.30 mmol for acrylic acid groups), followed by 1-[3-(dimethylamino)propyl]-3-ethylcarbodiimide methiodide (46 mg, 0.16 mmol, 0.5 equiv to the acrylic acid groups). The mixture was allowed to stir at room temperature for 10 min to ensure that the mixture became homogeneous. 2,2′-(Ethylenedioxy)bis(ethylamine) (23 mg, 0.16 mmol, 0.5 equiv to the acrylic acid groups) was dissolved in nanopure water (20 mL, 18 MΩ cm^{-1}) and added slowly over 10 min. The solution was allowed to stir at room temperature for 12 h before being transferred into dialysis tubing (MWCO = 6000–8000) and dialyzed against deionized water to remove all the byproducts. After 6 days, the solution was further dialyzed in nanopure water for 1 day. The final volume was about 195 mL, giving a polymer concentration of about 0.42 mg/mL.

RESULTS AND DISCUSSION

Block copolymers composed of segments of P*t*BA and PMA were selected as the starting points for the preparation of nanostructured materials containing hydrophilic and noncrosslinked core domains encased within hydrogel-like crosslinked networks. The synthetic design entailed four basic steps: (1) the selective cleavage of the *tert*-butyl ester functionalities afforded an amphiphilic block copolymer, (2) the remaining hydrophobic PMA portion of the chain allowed for the nucleation of nanoassemblies within an aqueous solution, (3) the amidation of the acrylic acid residues present within the corona of the assemblies established a stabilizing intra-assembly crosslinked network, and (4) the hydrolysis of the PMA side groups converted the core domain into hydrophilic PAA without detriment to the amide-based network linkages. Therefore, P*t*BA-*b*-PMA and PMA-*b*-P*t*BA were each prepared by sequential ATRP methods. The addition of PS chain segments, in the form of the triblock copolymer P*t*BA-*b*-PMA-*b*-PS, offered the somewhat surprising findings of nonspherical assemblies, and these nanostructures are highlighted in this report.

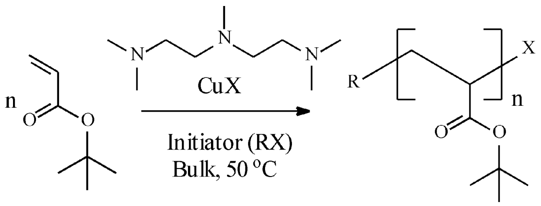

Scheme 1

2-EBP as an initiator and PMDETA/CuBr as a catalyst provided reaction conditions under which *t*BA polymerized smoothly at 50 °C in bulk to give well-defined homopolymers with polydispersities between 1.14 and 1.20 (Scheme 1 and Table I). The reaction mixture became progressively more viscous and solidified after about 80 min. Because the presence of Cu(II) can retard Cu(I)-mediated ATRP, the control of the amount of Cu(II) is im-

Table I. Homopolymerization of *t*BA and MA at 50 °C in Bulk

Entry	Monomer	Initiator	$[M]_0/[I]_0$	Time (min)	M_n^{calc} (g/mol)[a]	M_n^{NMR} (g/mol)	M_n^{GPC} (g/mol)	M_w/M_n	Conversion (%)[b]	Isolated Yield (%)	f[c]
1	*t*BA	2-EBP	100	75	11,000	7,000	12,100	1.14	86	76	0.92
2	*t*BA	1-EBB	100	85	12,300	9,600	13,500	1.27	96	74	0.91
3	*t*BA	2-EB*i*B	100	150	11,000	6,400	12,000	1.22	86	80	0.92
4	*t*BA	2-ECP	150	20	14,600	—	23,900	1.94	76	—	0.61
5	MA	2-EBP	150	75	8,300	8,700	9,110	1.04	64	55	0.90

[a] $M_n^{\mathrm{calc}} = ([M]/[I]_0) \cdot (\text{molecular weight of monomer}) \cdot (\%\ \text{conversion})$.
[b] Conversion determined from GPC.
[c] $f = M_n^{\mathrm{calc}}/M_n^{\mathrm{GPC}}$.

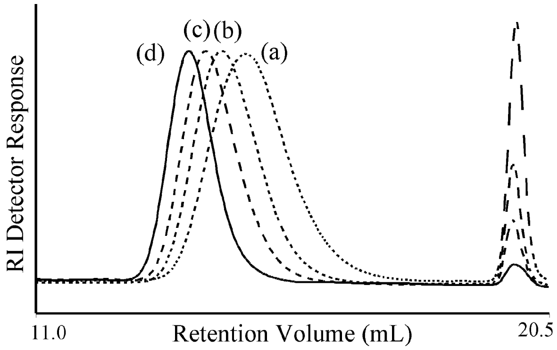

Figure 1. This composite of GPC eluograms illustrates the growth of the P*t*BA chain length and the concomitant reduction in the relative monomer concentration after the polymerization of *t*BA in bulk at 50 °C: (a) 55 min, $M_n^{GPC} = 4900$, $M_w/M_n = 1.29$; (b) 60 min, $M_n^{GPC} = 6630$, $M_w/M_n = 1.22$; (c) 70 min, $M_n^{GPC} = 8480$, $M_w/M_n = 1.18$; and (d) 75 min, $M_n^{GPC} = 9520$, $M_w/M_n = 1.17$. $[tBA]_0 = 6.8$ M; $[2\text{-EBP}]_0 = 67.7$ mM; $[\text{PMDETA}]_0 = 67.7$ mM; $[\text{CuBr}]_0 = 67.7$ mM.

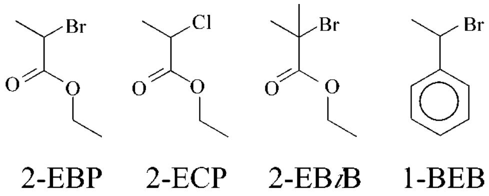

Figure 2. The initiators used for the ATRP-based polymerization of *t*BA included 2-EBP, 2-ECP, 2-EB*i*B, and 1-BEB.

portant. The addition of the monomers to a Schlenk flask containing CuBr at the temperature of liquid nitrogen, followed by degassing prior to the introduction of PMDETA ligand at 77 K, minimized the oxidation of Cu(I) to Cu(II) and produced acceptable polymerization rates. Monitoring of the polymerization by GPC showed nice control over the molecular weight growth and polydispersity (Fig. 1). At higher temperatures, for example, 90 °C, the polymerization rate of *t*BA was too fast; the reaction mixture solidified in less than 10 min, and the polydispersity was broad (PDI ~ 2). Therefore, the polymerizations were performed at 50 °C and, after the desired extent of conversion was achieved, were rapidly terminated by immersion of the reaction flask in liquid nitrogen to give the narrowest molecular weight dispersity. The polymer samples were isolated and purified by filtration through a plug of Al_2O_3 supported on a bed of celite or SiO_2, followed by repeated precipitations into methanol/water mixtures. SiO_2 alone was found to be inefficient for the removal of the copper catalyst from the reaction mixtures, allowing small amounts of copper salts to pass, even after repeated filtrations. However, basic Al_2O_3 on a thin layer of celite or SiO_2 effectively removed the copper salts.

Three other commonly used initiators, 1-bromoethylbenzene (1-BEB), 2-EB*i*B, and ethyl 2-chloropropionate (2-ECP; Fig. 2), were evaluated for the initiation of *t*BA at 50 °C. 1-BEB had the same reaction times as 2-EBP, yet polymers with broader PDIs were obtained. Slower initiation rates were observed with 2-EB*i*B, requiring longer polymerization times than 2-EBP, and the resulting polymers had slightly broader PDI values. In contrast, when 2-ECP was used as an initiator together with PMDETA/copper(I) chloride, the polymerization of *t*BA occurred at faster rates. At 50 °C, the reaction mixture became viscous quickly and solidified within 25 min. GPC analysis revealed a substantial concentration of dead chains. This can be explained by the lower solubility of $CuCl_2$ causing poor control over the reversible termination of the active chain ends or the higher bond energy between Cu and Cl shifting the equilibrium between the dormant and reactive species toward the reactive species. Either of these situations would lead to an increased propensity for termination reactions.

The application of the optimized conditions, involving the use of 2-EBP as an initiator and PMDETA/CuBr as a catalyst, to the polymerization of MA also gave smooth polymerizations at 50 °C in bulk and yielded well-defined PMA homopolymers (Scheme 2). GPC analyses showed nice control over the molecular weights and polydispersities throughout the polymerization (Fig. 3). MALDI-TOF mass spectrometry allowed for the determination of the absolute molecular weights and the polydispersities (Fig. 4). The mass difference between the neighboring peaks was 86 Da, corresponding to the repeat unit of MA. Again, termination of the polymerization via the immersion of the flask into liquid nitrogen to

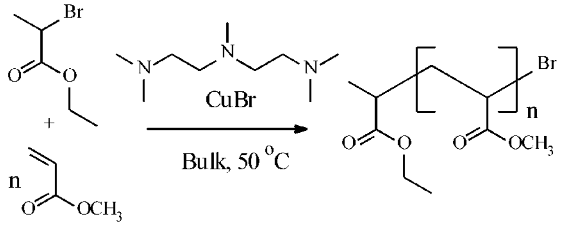

Scheme 2

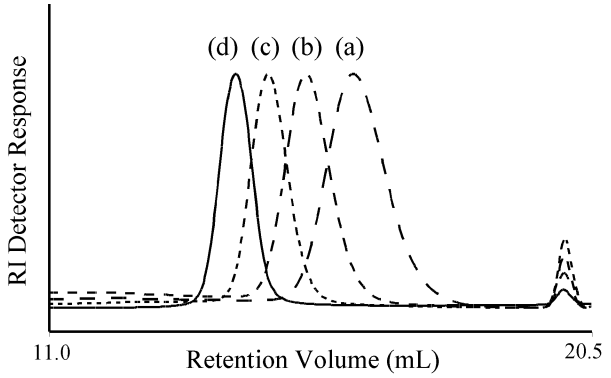

Figure 3. This composite of GPC eluograms illustrates the growth of the PMA chain length and the concomitant reduction in the relative monomer concentration after the polymerization of MA at 50 °C in bulk: (a) 20 min, $M_n^{\mathrm{GPC}} = 1580$, $M_w/M_n = 1.13$; (b) 45 min, $M_n^{\mathrm{GPC}} = 3080$, $M_w/M_n = 1.07$; (c) 60 min, $M_n^{\mathrm{GPC}} = 5320$, $M_w/M_n = 1.05$; and (d) 75 min, $M_n^{\mathrm{GPC}} = 9110$, $M_w/M_n = 1.04$. $[\mathrm{MA}]_0 = 10.8$ M; $[\text{2-EBP}]_0 = 72.3$ mM; $[\mathrm{PMDETA}]_0 = 72.3$ mM; $[\mathrm{CuBr}]_0 = 72.3$ mM.

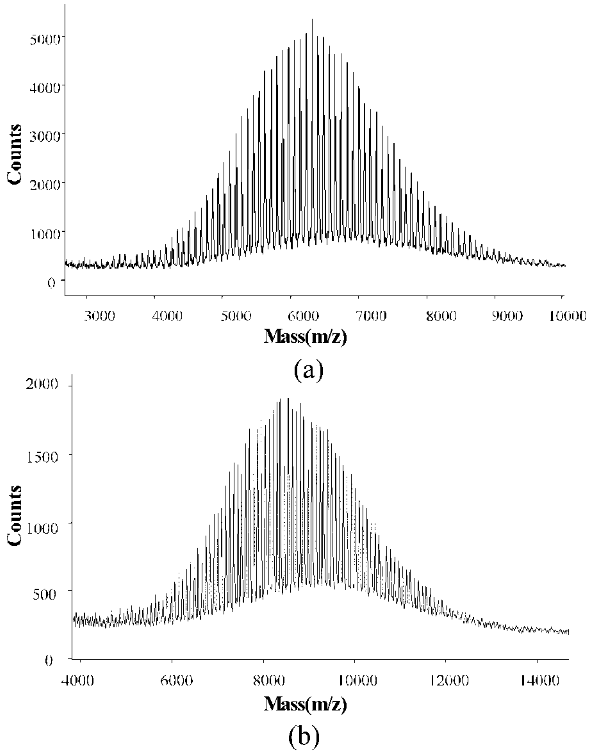

(a)

(b)

Figure 4. MALDI-TOF spectra acquired from PMA samples dispersed in a matrix of 3-indole acrylic acid doped with silver acetate: (a) $M_n = 6268$, $M_w/M_n = 1.031$ and (b) $M_n = 8598$, $M_w/M_n = 1.030$.

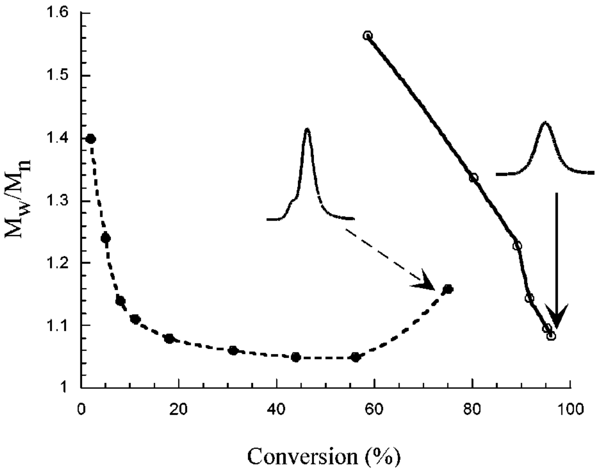

Figure 5. Polydispersity versus conversion for the polymerizations of MA (dashed line) and *t*BA (solid line). The insets show the GPC peak shapes for the polymers at the highest extents of conversion.

quench all chain growth at the same time gave the narrowest polydispersity value. The narrow polydispersities ($M_w/M_n = 1.030$) measured by MALDI-TOF agreed with the GPC results ($M_w/M_n = 1.04$).

The techniques developed for the careful control of the reaction conditions allowed for the polymerizations of *t*BA and MA, employing 2-EBP as an initiator and PMDETA/CuBr as a catalyst at 50 °C in bulk, to be performed on relatively large scales (90 g for *t*BA and 120 g for MA) with results similar to those for the small-scale polymerizations (5–10 g). During the polymerization of *t*BA, the polydispersity decreased with increasing conversion, and homopolymer coupling was not common. As for MA, the polydispersity was most narrow between 40 and 60% conversions;[36] slight increases in the PDI values were observed at higher conversions. In comparison with the polymerizations at higher temperatures, where homopolymer coupling was very common at high conversions, much less homopolymer coupling was observed at 50 °C (Fig. 5). A study of the kinetics of *t*BA polymerization revealed a linear increase in $\ln([\mathrm{M}]_0/[\mathrm{M}])$ with time, which is consistent with the presence of a constant number of propagating species during the polymerization (Fig. 6).

The stereochemistry (tacticity) of the homopolymers was determined by ^{1}H NMR (in $\mathrm{CDCl_3}$) via a comparison of the intensities of the downfield meso proton signal (δ 1.8–2.0 ppm) with the methine proton resonance (δ 2.2–2.4 ppm).[42] Both P*t*BA and PMA homopolymers obtained under the ATRP reaction conditions were atactic ($m/r = 50/50$).

The preparation of P*t*BA-*b*-PMA diblock copolymers was accomplished by the polymerization of

MA from the P*t*BA macroinitiators in bulk at 50 °C and in toluene at 90 °C, with no significant difference (Scheme 3). Because toluene is a good solvent for both P*t*BA and PMA, it was chosen to be the solvent for the solution polymerization, and the conditions employed were similar to those for the homopolymer preparations. As much as 80 vol % toluene could be used to dissolve the P*t*BA macroinitiator, and although fine particles could be seen toward the late stages of the polymerization, the heterogeneity did not adversely affect the polymerization. The initiation and propagation also proceeded smoothly in bulk, giving diblock copolymers with narrow molecular weight dispersities (Table II). The bulk polymerizations could be taken to relatively high conversions without polymer chain coupling, unless the polymerization mixture was allowed to remain at elevated temperatures for periods of time beyond solidification. MALDI-TOF mass spectra were obtained for some of the diblocks (Fig. 7). Because the diblock spectra contained two distributions, having mass differences of 86 and 128 Da due to MA and *t*BA repeat units, respectively, the peak shapes were not as well resolved as for the PMA homopolymer (Fig. 4). The PDI values calculated from the MALDI-TOF data were similar to those obtained from GPC.

A second route for the preparation of diblock copolymers composed of *t*BA and MA involved the initial polymerization of MA followed by the growth of *t*BA from the PMA macroinitiator (Scheme 4). Because the T_g of PMA is low (~10 °C), PMA was first frozen in liquid nitrogen and broken into small pieces for convenient measurement and transfer. However, if the macroinitiator was not pumped under vacuum long enough, the moisture that condensed during the aforementioned procedure caused a color change of the reaction mixture from the normal green to bright blue. This was easily remedied by the removal of all water from the reaction mixture by azeotroping with toluene. The amount of CuBr employed during the polymerization was critical. If an insufficient amount was used, in comparison to the molar equivalents of active bromoalkyl chain ends on the macroinitiator, incomplete initiation was observed, and the amount of homopolymer contamination was inversely proportional to the amount of CuBr used. At 1 equiv of CuBr or more, clean initiation was observed, as demonstrated by the GPC eluograms of Figure 8.

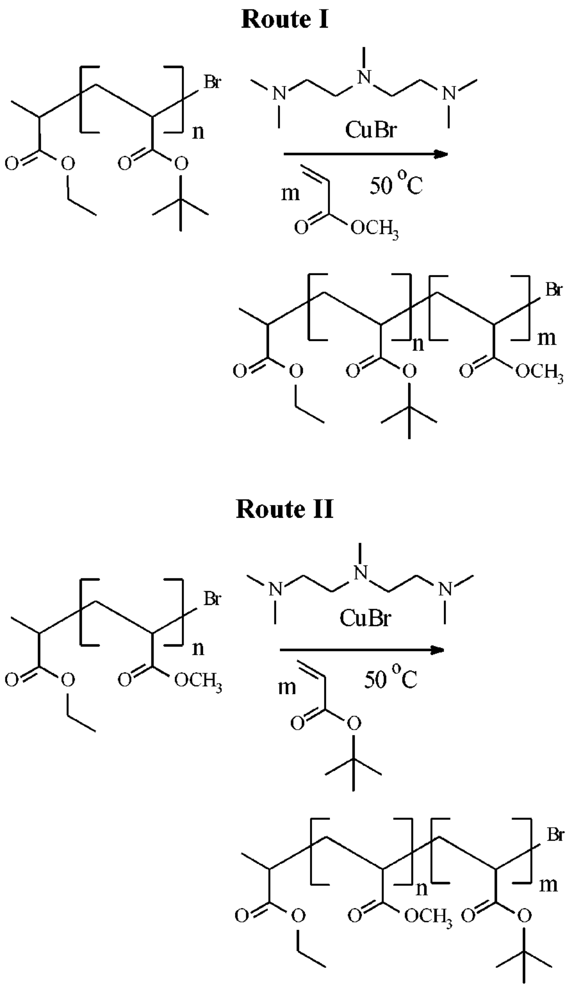

Scheme 3

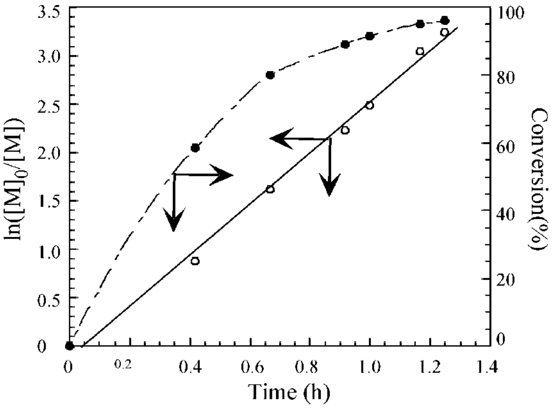

Figure 6. Kinetics of the bulk polymerization of *t*BA at 50 °C. $[tBA]_0/[PMDETA]_0/[CuBr]_0 = 100/1/1$; $[tBA]_0 = 6.8$ M; $[2\text{-EBP}]_0 = 67.7$ mM; $[CuBr]_0 = 67.7$ mM; $[PMDETA]_0 = 67.7$ mM.

Selective cleavage of the *tert*-butyl ester groups in the presence of methyl esters was achieved by the diblock copolymers being treated in dichloromethane with anhydrous TFA at room temperature. The reaction was monitored by ^{1}H NMR

Table II. Diblock and Triblock Copolymers Prepared by ATRP with Copper(I) Bromide/PMDETA

Entry	Macroinitiator [I]	Monomer	[CuBr]/[I]	Solvent	T (°C)	Time (h)	$(M_n)_{\text{expt}}$	$(M_n)_{\text{GPC}}$	M_w/M_n
1	P*t*BA	Styrene	1.1	Toluene[a]	60	4.5	12,100[d]	16,100	1.22
2	P*t*BA	MA	1.4	Toluene[b]	90	2.5	16,800[d]	18,500	1.11
3	P*t*BA	MA	3.0	None	50	2.7	30,217[e]	32,300	1.19[e]
4	P*t*BA	MA	3.0	None	50	2.0	14,875[e]	18,500	1.09[e]
5	PMA	*t*-BA	0.9	Toluene[c]	90	12.5	—	22,800	1.30
6	PMA	*t*-BA	0.7	Toluene[c]	90	11.0	—	16,800	1.33
7	PMA	*t*-BA	2.0	Toluene[c]	90	10.7	12,000[d]	18,700	1.17
8	P*t*BA-*b*-PMA	Styrene	2.2	Toluene[c]	90	7.5	—	30,400	1.23
9	P*t*BA-*b*-PMA	Styrene	3.9	None	50	6.7	20,000[d]	28,700	1.16

[a] 43% by volume.
[b] 80% by volume.
[c] 50% by volume.
[d] By ^{1}H NMR end-group analysis.
[e] By MALDI-TOF measurement.

(Fig. 9). The signal at δ 1.49 ppm, resulting from the *tert*-butyl protons of the P*t*BA block, decreased in intensity, whereas the signal at δ 1.62 ppm, corresponding to the *tert*-butyl trifluoroacetate product, appeared and increased in intensity. After 3 h, the *tert*-butyl ester signal at δ 1.49 ppm had nearly disappeared, and the signal from the P*t*BA block backbone at δ 2.4 ppm shifted downfield to δ 2.5 ppm. Extended reaction times (overnight) were often used to ensure the completion of the *tert*-butyl ester conversion to PAA chain segments. The methyl ester functional groups of the PMA blocks and the end groups of the copolymer remained intact even after 60 h, as was observed in a comparison of their proton resonance signals and those of the internal standard, bromobenzene.

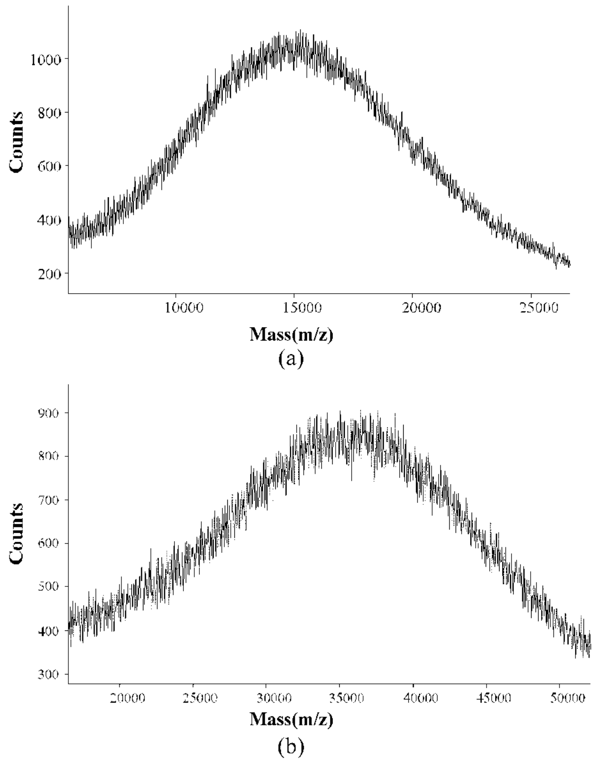

Figure 7. MALDI-TOF spectra of P*t*BA-*b*-PMA diblock copolymers dispersed in a matrix of 3-indole acrylic acid doped with silver acetate: (a) M_n = 14,875, M_w/M_n = 1.09 and (b) M_n = 30,217, M_w/M_n = 1.19.

Differential scanning calorimetry was used to evaluate the thermal transition temperatures for the homopolymers and block copolymers. T_g's were observed for PMA at 10 °C and for P*t*BA at 34 °C. The diblock copolymer, P*t*BA-*b*-PMA, exhibited two T_g's at 15 and 44 °C for the immiscible PMA and PtBA phases, respectively. After the conversion of the P*t*BA block to yield PAA-*b*-PMA, T_g's were observed at 10 °C for PMA and 114 °C for PAA, clearly indicating that the two phases were immiscible.

A P*t*BA-*b*-PMA-*b*-PS triblock copolymer was also synthesized in bulk at 50 °C in the presence

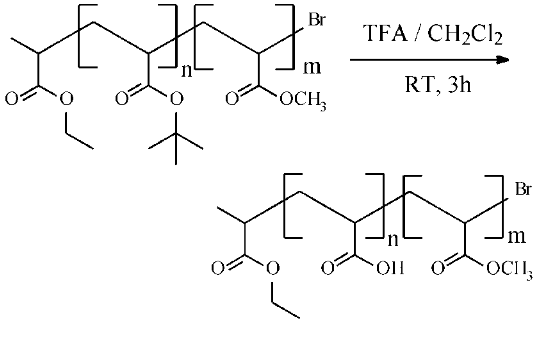

Scheme 4

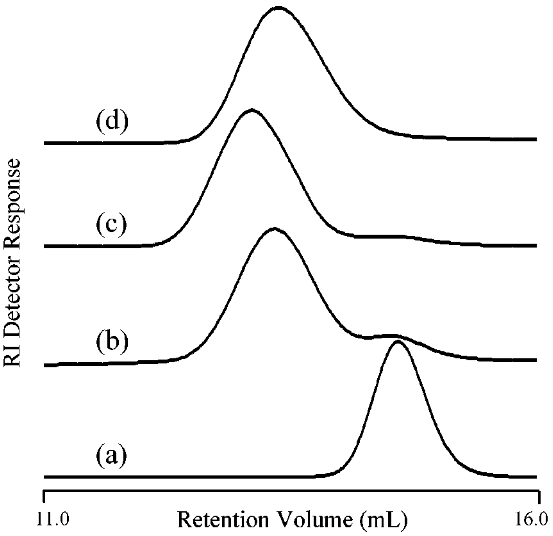

Figure 8. GPC traces illustrate the effects that different amounts of CuBr catalyst had on the initiation of *t*BA as a second block from PMA as a macroinitiator in toluene at 90 °C: (a) PMA as a macroinitiator, $M_n^{\mathrm{GPC}} = 6610$, $M_w/M_n = 1.04$; (b) 0.7 equiv of CuBr to the macroinitiator to give PMA-*b*-P*t*BA, $M_n^{\mathrm{GPC}} = 16{,}800$, $M_w/M_n = 1.33$; (c) 0.9 equiv of CuBr to the macroinitiator to give PMA-*b*-P*t*BA, $M_n^{\mathrm{GPC}} = 22{,}800$, $M_w/M_n = 1.30$; and (d) 2 equiv of CuBr to the macroinitiator to give PMA-*b*-P*t*BA, $M_n^{\mathrm{GPC}} = 18{,}700$, $M_w/M_n = 1.17$.

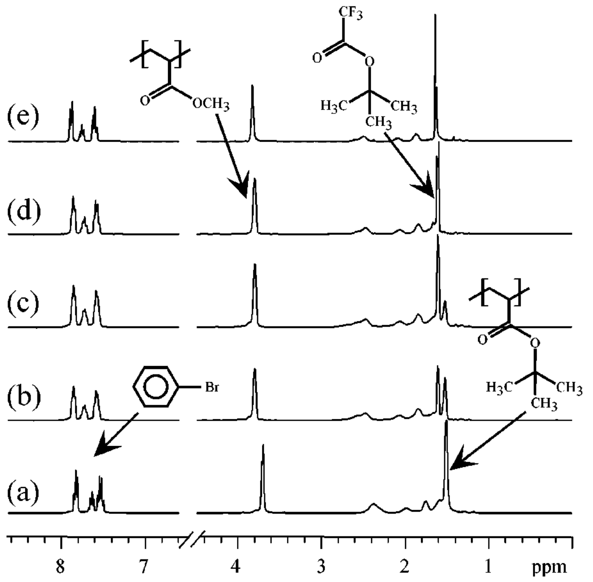

Figure 9. A time-course ^{1}H NMR study monitored the selective cleavage of the *tert*-butyl esters of P*t*BA-*b*-PMA via a reaction with TFA (3 equiv with respect to the *tert*-butyl ester groups) at room temperature: (a) the diblock copolymer in CD_2Cl_2 (bromobenzene was added as an internal standard) at (b) 20 min, (c) 60 min, (d) 120 min, and (e) 60 h after the addition of TFA.

of CuBr/PMDETA, with the growth of the third (PS) block occurring from the diblock copolymer, P*t*BA-*b*-PMA, bearing a bromoalkyl chain end as a result of the ATRP method of preparation (Scheme 5). Under these reaction conditions, styrene could be polymerized at 50 °C in bulk or at 60 °C in toluene, albeit at significantly slower polymerization rates than were observed with MA and *t*BA monomers. Also, substantial amounts of products resulting from polymer chain coupling were observed after the polymerization of styrene from the P*t*BA-*b*-PMA macroinitiator in toluene at 90 °C when taken to high conversion (Fig. 10).

Cleavage of the *tert*-butyl ester groups of the P*t*BA-*b*-PMA-*b*-PS triblock copolymer was then performed via reaction with anhydrous TFA in dichloromethane at room temperature to afford the amphiphilic PAA-*b*-PMA-*b*-PS triblock copolymer. A previously reported procedure[15] was employed for the assembly of micelles in water, which were then stabilized with a water-soluble carbodiimide, 1-[3-(dimethylamino)propyl]-3-ethylcarbodiimide methiodide, to activate the acrylic acid groups present within the shell, followed by crosslinking with a diamine, 2,2′-(ethylenedioxy)-bis(ethylamine), to form SCK nanostructured materials (Fig. 11).

In addition to spherical particles, cylindrically shaped nanostructures were formed. The deposition of aqueous solutions containing the mixtures of nanospheres and nanocylinders onto a mica substrate, followed by the sample being allowed to dry freely in air, and an analysis by AFM revealed very interesting segregation phenomena as a function of particle topology. The spheres organized into hexagonally packed monolayers in contact with the mica, whereas the cylinders preferred to assemble on the surface generated by the spherical particles [Fig. 12(a–c)]. This ordering occurred over long ranges, regardless of the

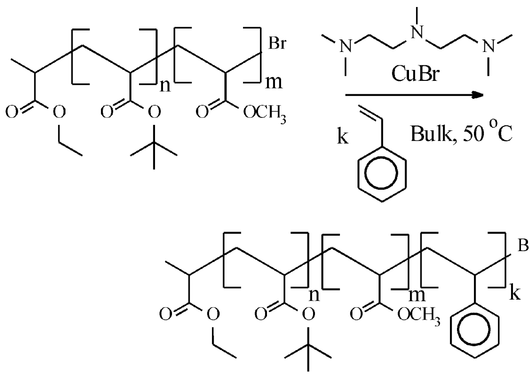

Scheme 5

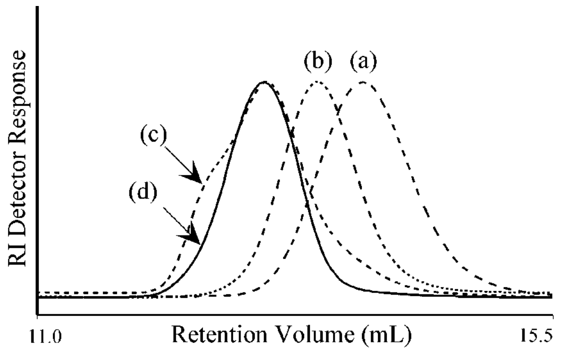

Figure 10. GPC eluograms of (a) P*t*BA as the macroinitiator, $M_n^{GPC} = 12{,}100$, $M_w/M_n = 1.14$; (b) P*t*BA-*b*-PMA as the macroinitiator, $M_n^{GPC} = 18{,}500$, $M_w/M_n = 1.11$; (c) P*t*BA-*b*-PMA-*b*-PS, $M_n^{GPC} = 30{,}400$, $M_w/M_n = 1.23$, resulting from the polymerization of the third (PS) segment at 90 °C in toluene; and (d) P*t*BA-*b*-PMA-*b*-PS, $M_n^{GPC} = 28{,}700$, $M_w/M_n = 1.16$, resulting from the polymerization of the third (PS) segment at 50 °C in bulk.

solution concentration of the nanostructures [compare the images of Fig. 12(a,b)]. Section analysis of the AFM images determined that the spheres and cylinders were each of comparable heights (15 ± 2 nm); however, the cylinder lengths extended from 50 nm to 2 μm (Fig. 13). Further work is required to control the assembly processes to generate well-defined nanostructures of a variety of shapes and morphologies and also to understand the complex surface interactions that drive their segregation behaviors.

Preliminary experiments were performed, utilizing the AFM tip as a manipulation tool to examine the mechanical integrity of the SCK nanocylinders. After tapping-mode AFM imaging was used to visualize the nanostructures, the probe tip was brought into contact with the mica at the position indicated by the arrowhead in Figure 14(a). In this example, a bent cylinder was subjected to contact-mode AFM scanning to allow for the AFM tip to exert lateral force on the nanostructure. After the tip manipulation, tapping-mode AFM was resumed to collect the image of the same sample region [Fig. 14(b)]. Rather than stretching or being moved across the substrate, the nanostructure instead ruptured. This behavior was observed several times and suggests that the shell thickness and extent of crosslinking in this system did not provide sufficient networking to overcome some combination of the attractive forces with the mica substrate and the local forces applied by the AFM tip.

CONCLUSIONS

After intending to produce entirely hydrophilic nanostructured materials as stable entities with

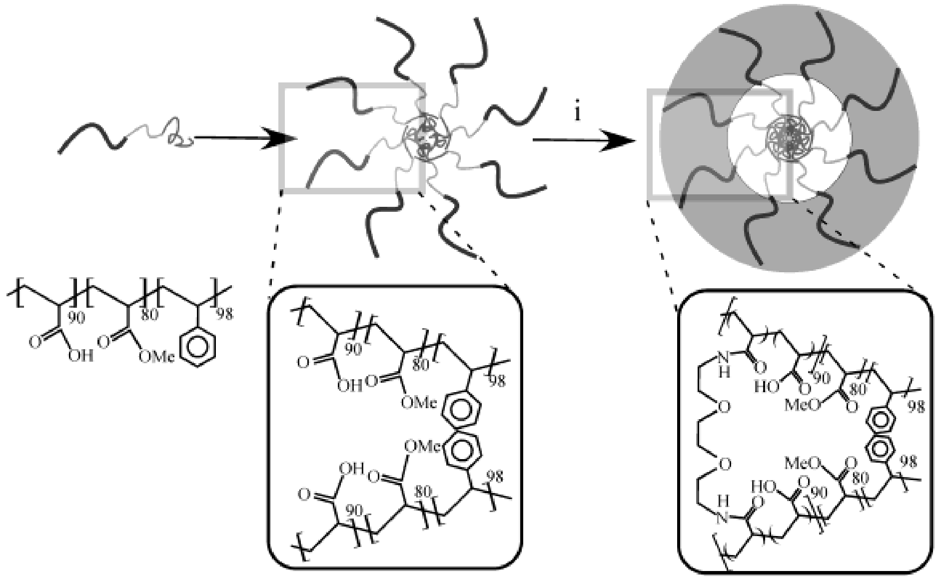

Figure 11. The general strategy for the preparation of SCK nanostructures involves the formation of micelles from PAA-*b*-PMA-*b*-PS in water and subsequent amidation reactions between the acrylic acid residues of the peripheral chain segments and diamino crosslinkers: (i) 1-[3-(dimethylamino)propyl]-3-ethylcarbodiimide methiodide and 2,2′-(ethylenedioxy) bis(ethylamine).

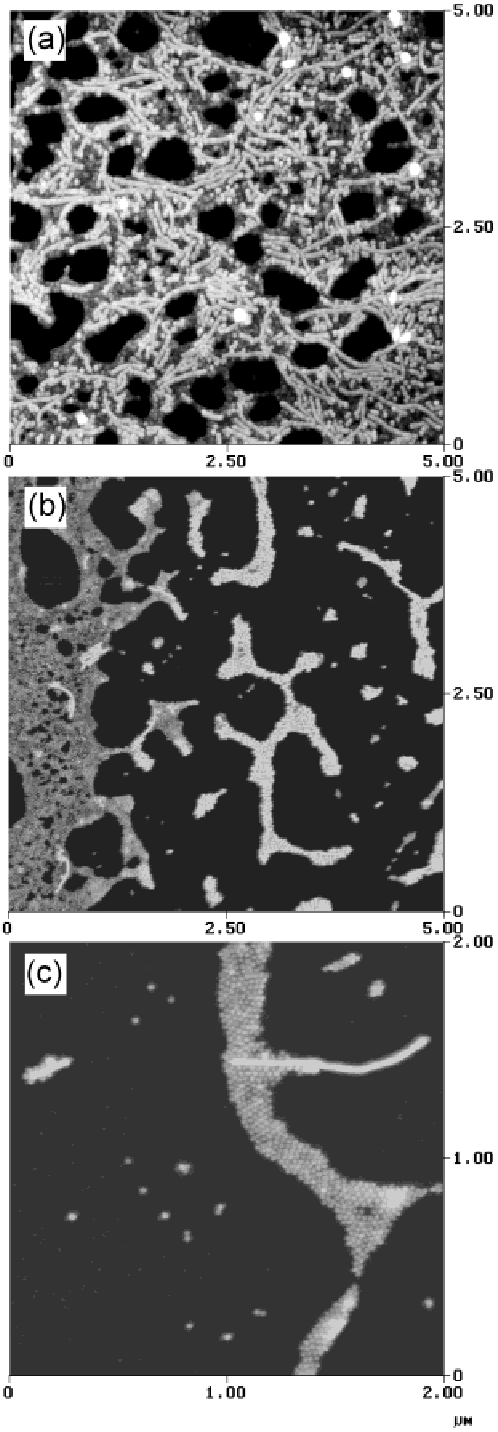

Figure 12. Tapping-mode AFM images of SCK nanostructures that were deposited from an aqueous solution onto mica substrates and then allowed to dry reveal interesting segregation behaviors. The concentrations of the aqueous solutions of the nanostructures were (a) 0.4 mg/mL, (b) 0.08 mg/mL, and (c) 0.08 mg/mL (imaged at 2 × 2 μm).

complex morphologies within water, we encountered interesting chemistry in (1) the methodology of ATRP-based techniques for the production of well-defined diblock and triblock copolymers incorporating acrylate monomers, (2) their transformation into nanostructured materials of mixed topologies, (3) the topology-driven segregation of those nanostructures, and (4) the evaluation of the mechanical integrity of single nanoscale materials. Further study is required to gain control over the formation of complex nanostructured materials from triblock copolymers, employing

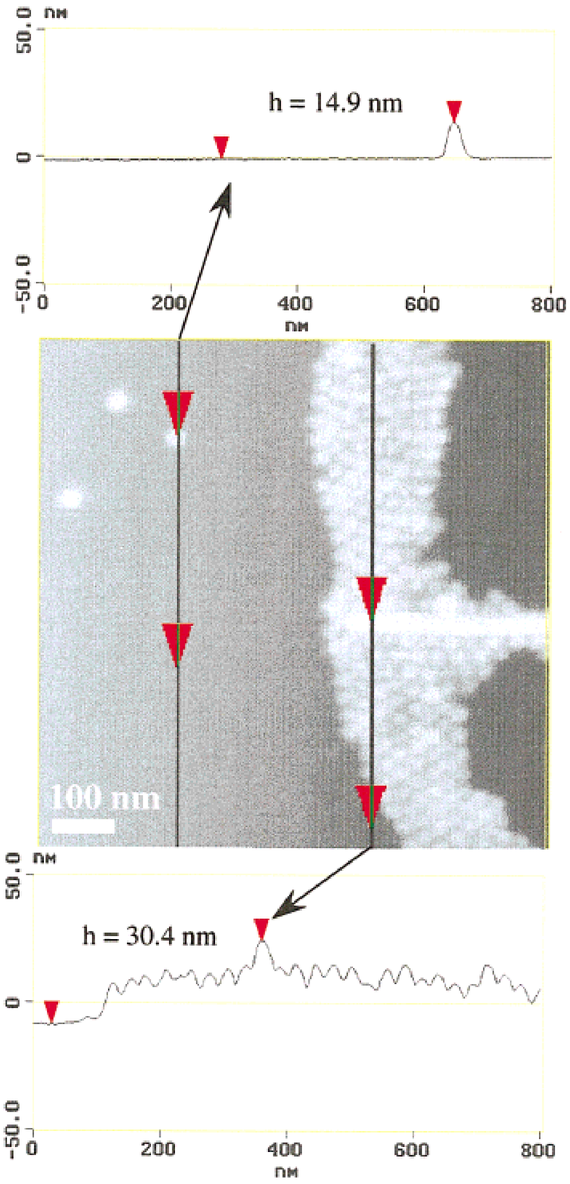

Figure 13. Section analysis on an expanded area of the AFM image from Figure 12. (c). A single sphere has a height of 14.9 nm, whereas the combined rod and spheres lying below have a height of 30.4 nm.

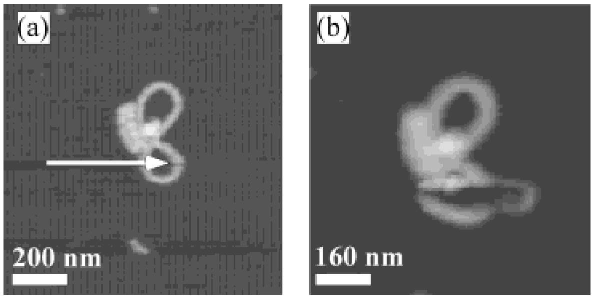

Figure 14. Tapping-mode AFM images of SCK nanostructures on mica, prepared by the deposition of a 0.05 mg/mL solution concentration (a) before manipulation with the AFM tip (the arrow indicates the location at which the tip was brought into contact with the mica for the mechanical manipulation) and (b) after the AFM tip was brought into contact with the mica substrate at the position noted by the arrowhead and scanned to the right in contact mode to exert lateral force on the nanostructure.

the general methodology of self-assembly in solution followed by covalent stabilization. Advanced tools will be needed to characterize their surface interactions and mechanical properties. Additionally, chemical modification and mechanical manipulation of such nanostructures will be further explored.

Funding of this research by the National Science Foundation (DMR-9974457) is gratefully acknowledged. The authors also thank Mr. Yensheng Wang and Professor Michael L. Gross for the MALDI-TOF measurements. The Washington University Mass Spectrometry Facility is supported by the National Institutes of Health, National Center for Research Resources (Grant No. P41RR0954).

REFERENCES AND NOTES

1. Zhang, L.; Eisenberg, A. Science 1995, 268, 1728–1731.
2. Zhang, L.; Eisenberg, A. J Am Chem Soc 1996, 118, 3168–81.
3. Saito, R.; Akiyama, Y.; Tanaka, M.; Ishizu, K. Colloids Surf A 1999, 153, 305–310.
4. Bütün, V.; Wang, X. S.; Banez, M. V. D. P.; Robinson, K. L.; Billingham, N. C.; Armes, S. P.; Tuzar, Z. Macromolecules 2000, 33, 1–3.
5. Bütün, V.; Lowe, A. B.; Billingham, N. C.; Armes, S. P. J Am Chem Soc 1999, 121, 4288–4289.
6. Discher, B. M.; Won, Y.-Y.; Ege, D. S.; Lee, J. C. M.; Bates, F. S.; Discher, D. E.; Hammer, D. A. Science 1999, 284, 1143–1146.
7. Sanji, T.; Nakatsuka, Y.; Kitayama, F.; Sakurai, H. Chem Commun 1999, 2201–2202.
8. Sukegawa, M.; Irizato, Y.; Ishitoku, T.; Machida, K.; Fukawa, S.; Katoh, T.; Tamatani, H.; Fukuoka, A. Biodegradable Core–Shell Particles Containing Crosslinked Polyamino Acids and Their Manufacture and Use in Hygienic Products or Soil Moisturizers; PCT Int. Appl. WO 0027904, 2000.
9. Thurmond, K. B., II; Kowalewski, T.; Wooley, K. L. J Am Chem Soc 1996, 118, 7239–7240.
10. Caruso, F.; Schueler, C.; Kurth, D. G. Chem Mater 1999, 11, 3394–3399.
11. Hamers, C.; Rupaner, R.; Leyrer, R. J.; Schuhmacher, P.; Yang, Z. Pigmented Dispersions of Core–Shell Polymer Particles for Manufacture of Coatings; Ger. Offen. DE 98-19834194, 2000.
12. Wooley, K. L. J Polym Sci Part A: Polym Chem 2000, 38, 1397–1407.
13. Thurmond, K. B., II; Remsen, E. E.; Kowalewski, T.; Wooley, K. L. Nucleic Acids Res 1999, 27, 2966–2971.
14. Huang, H.; Remsen, E. E.; Kowalewski, T.; Wooley, K. L. J Am Chem Soc 1999, 121, 3805–3806.
15. Huang, H.; Wooley, K. L.; Remsen, E. E. Chem Commun 1998, 1415–1416.
16. Wooley, K. L.; Huang, H.; Kowalewski, T. Polym Mater Sci Eng 1999, 80, 13.
17. Zhang, Q.; Remsen, E. E.; Wooley, K. L. J Am Chem Soc 2000, 122, 3642–3651.
18. Percec, V. Polymerization of Free Radically Polymerizable Vinyl Monomers Using Sulfonyl Halides and Transition Metal Compounds as Initiators; PCT Int. Appl. WO 9820050, 1998.
19. Sawamoto, M.; Kamigaito, M. J Macromol Sci Pure Appl Chem 1997, 34, 1803–1814.
20. Matyjaszewski, K.; Patten, T. E.; Xia, J. J Am Chem Soc 1997, 119, 674–680.
21. Matyjaszewski, K.; Coca, S.; Gaynor, S. G.; Wei, M.; Woodworth, B. E. Macromolecules 1997, 30, 7348–7350.
22. Matyjaszewski, K.; Coca, S.; Gaynor, S. G.; Wei, M.; Woodworth, B. E. Macromolecules 1998, 31, 5967–5969.
23. Matyjaszewski, K.; Nakagawa, Y.; Jasieczek, C. B. Macromolecules 1998, 31, 1535–1541.
24. Benoit, D.; Chaplinski, V.; Braslau, R.; Hawker, C. J. J Am Chem Soc 1999, 121, 3904–3920.
25. Hawker, C. J.; Barclay, G. G.; Dao, J. J Am Chem Soc 1996, 118, 11467–11471.
26. Hawker, C. J.; Barclay, G. G.; Orellana, A.; Dao, J.; Devonport, W. Macromolecules 1996, 29, 5245–5254.
27. Chiefari, J.; Chong, Y. K.; Ercole, F.; Krstina, J.; Jeffery, J.; Le, T. P. T.; Mayadunne, R. T. A.; Meijs, G. F.; Moad, C. L.; Moad, G.; Rizzardo, E.; Thang, S. H. Macromolecules 1998, 31, 5559–5562.
28. Chong, Y. K.; Le, T. P. T.; Moad, G.; Rizzardo, E.; Thang, S. H. Macromolecules 1999, 32, 2071–2074.
29. Mayadunne, R. T. A.; Rizzardo, E.; Chiefari, J.; Chong, Y. K.; Moad, G.; Thang, S. H. Macromolecules 1999, 32, 6977–6980.

30. Mayadunne, R. T. A.; Rizzardo, E.; Chiefari, J.; Krstina, J.; Moad, G.; Postma, A.; Thang, S. H. Macromolecules 2000, 33, 243–245.
31. Xia, J.; Matyjaszewski, K. Macromolecules 1997, 30, 7697–7700.
32. Davis, K. A.; Paik, H.-J.; Matyjaszewski, K. Macromolecules 1999, 32, 1767–1776.
33. Coca, S.; Jasieczek, C. B.; Beers, K. L.; Matyjaszewski, K. J Polym Sci Part A: Polym Chem 1998, 36, 1417–1424.
34. Percec, V.; Barboiu, B.; Neumann, A.; Ronda, J. C.; Zhao, M. Macromolecules 1996, 29, 3665–3668.
35. Wang, J.-L.; Grimaud, T.; Shipp, D. A.; Matyjaszewski, K. Macromolecules 1998, 31, 1527–1534.
36. Wang, J.-S.; Matyjaszewski, K. Macromolecules 1995, 28, 7901–7910.
37. Patten, T. E.; Xia, J.; Abernathy, T.; Matyjaszewski, K. Science 1996, 272, 866–868.
38. Jankova, K.; Kops, J.; Chen, X.; Batsberg, W. Macromol Rapid Commun 1999, 20, 219–223.
39. Davis, K. A.; Matyjaszewski, K. Macromolecules 2000, 33, 4039–4047.
40. Zhang, X.; Xia, J.; Matyjaszewski, K. Macromolecules 2000, 33, 2340–2345.
41. Burguiere, C.; Pascual, S.; Coutin, B.; Polton, A.; Tardi, M.; Charleux, B.; Matyjaszewski, K.; Vairon, J.-P. Macromol Symp 2000, 150, 39–44.
42. Liu, W.; Nakano, T.; Okamoto, Y. J Polym Sci Part A: Polym Chem 2000, 38, 1024–1032.